Mines Branch Information Circular IC 299

THE PHYSICAL METALLURGY OF QUENCHED AND TEMPERED LOW-CARBON STEEL, WITH SPECIAL REFERENCE TO LARGE DIAMETER LINE PIPE APPLICATIONS

by

J. D. Boyd*

ABSTRACT

This report summarizes the present state of the art of the physical metallurgy of line pipe steels and considers the possibilities for developing new high-strength, high-toughness grades of steel suitable for arctic pipelines. It is suggested that, for large-diameter, heavy-walled line pipe in which 80 to 100-ksi (550 to 690-MN/m^2) yield strength is required, quenched and tempered low-carbon steels ($\leq$0.10C) offer an attractive combination of strength, toughness, formability, weldability, and economy of production. Two possible methods for manufacturing line pipe incorporating a quench and temper process are outlined, and the techniques for controlling microstructure are discussed for both methods. Finally, the relations between the microstructure of quenched and tempered low-carbon steel and two important mechanical properties are discussed in detail. The mechanical properties which are considered are the basic strengthening mechanisms and the origins of fracture toughness, with particular reference to dynamic toughness.

---

*Research Scientist, Ferrous Metals Section, Physical Metallurgy Division, Mines Branch, Department of Energy, Mines and Resources, Ottawa, Canada.

Direction des mines

Circulaire d'information IC 299

LA MÉTALLURGIE PHYSIQUE DE L'ACIER TREMPÉ ET REVENU À BASSE TENEUR EN CARBONE AVEC UNE RÉFÉRENCE SPÉCIALE AUX APPLICATIONS DU TUYAU DE CONDUITE A LARGE DIAMETRE

par

J.D. Boyd*

RÉSUMÉ

Dans ce rapport, l'auteur donne un résumé de l'état actuel de l'art de la métallurgie physique des aciers utilisés pour les tuyaux de conduite et il considère les possibilités pour développer l'acier de qualité à haute résistance et à haute ténacité convenable pour les pipelines arctiques. Pour un pipeline à large diamètre et de forte épaisseur dans lequel la limite d'élasticité de 80 à 100-ksi (550 à 690-MN/m^2) est nécessaire, l'auteur suggère que les aciers trempés et revenus à base teneur en carbone (<0.10C) offrent une combinaison attrayante de résistance, de ténacité, de ductilité, de soudabilité et d'économie de production. Il donne les généralités sur deux méthodes possibles pour la fabrication du tuyau de conduite qui incorpore un procédé de trempe et de revenu et il discute aussi des techniques pour contrôler la microstructure pour les deux méthodes. Dernièrement, il discute en détail les rapports entre la microstructure de l'acier trempé et revenu à basse teneur en carbone et les deux propriétés mécaniques importantes. L'auteur considère que les propriétés mécaniques sont les mécanismes résistants de base et les origines de la ténacité de fracture, avec une référence particulière à la ténacité dynamique.

---

*Chercheur scientifique, Section des métaux non ferreux, Division de la métallurgie physique, Direction des mines, ministère de l'Énergie, des Mines et des Ressources, Ottawa, Canada.

INTRODUCTION

The design and construction of pipelines to transport natural gas from the Canadian Arctic present a formidable challenge to the materials engineer. The massive capital outlay required for such a project demands that a serious effort be made to identify the most economical material and manufacturing technique for the line pipe. Obviously, the most efficient transmission of the gas is achieved with the largest diameter pipe operating at the highest pressure. Thus, there is an impetus to develop both higher-strength line pipe materials and the capability to manufacture large-diameter pipe. The achievement of these two goals is limited by several factors. Firstly, the fracture toughness of the line pipe material is of paramount importance; service conditions in the Arctic will be more severe than previously encountered for gas transmission lines, and a pipeline failure there would be expensive to repair. Secondly, the line pipe must be such that it can be welded by conventional techniques under arctic conditions. Finally, there is the over-riding constraint of cost which pervades every step of the operation from the production of the line pipe material to the installation of the pipeline itself. Thus, the materials engineer is faced with a classical materials selection problem -- he must achieve certain stringent mechanical-property criteria at the lowest possible cost. This report summarizes the present state of the art of the physical metallurgy of line pipe steels and considers the possibilities for developing new high-strength, high-toughness grades of steel suitable for arctic pipelines.

CURRENT TRENDS IN LINE PIPE STEELS

A large-diameter line pipe product, which is representative of those currently produced, would be 40-in. (1.02-m) diameter, 0.40-in. (10.2-mm) wall thickness pipe manufactured to either CSA Standard Z245.2 - Grade 65 or API Standard 5LX65. These standards require, in part, 65-ksi (450-MN/m^2) yield strength, 80-ksi (550-MN/m^2) ultimate strength, 20% tensile elongation over a 2-in. (50.8-mm) gauge length, and (sometimes) an average shear area of at least 75% in the Drop Weight Tear Test (DWTT). These property requirements are usually met by using a grain-refined, carbon-manganese-niobium steel in the controlled-rolled condition. The published compositions of some representative steels are given in Table 1. This material has a fine-grained, polygonal, ferrite-pearlite microstructure, which is illustrated in Figure 1(a).

Current development work in line pipe steel is concentrating on improving the controlled-rolling techniques[1-3]. The trend is towards lower carbon contents and higher percentages of alloy elements such as niobium, vanadium, molybdenum, and chromium. The published compositions of some steels which are being developed are given in Table 2. The alloy elements, niobium in particular, retard the recrystallization and grain growth of austenite and depress the austenite-to-ferrite transformation temperature. The result is an extremely fine, ferrite-carbide microstructure, which can have a non-polygonal morphology (Figure 1(b)). Additional strengthening is provided by an unrecovered dislocation substructure and by precipitation of alloy carbides within the ferrite grains[1-6]. It is expected that this type of steel will be used for 50 to 60-in. (1.25 to 1.52-m) diameter, 0.50 to 0.75-in. (12.7 to 19.0-mm) wall thickness pipe manufactured to a Grade 70 (X70) Standard. In many cases a spiral weld process will be employed in the manufacture of the pipe.

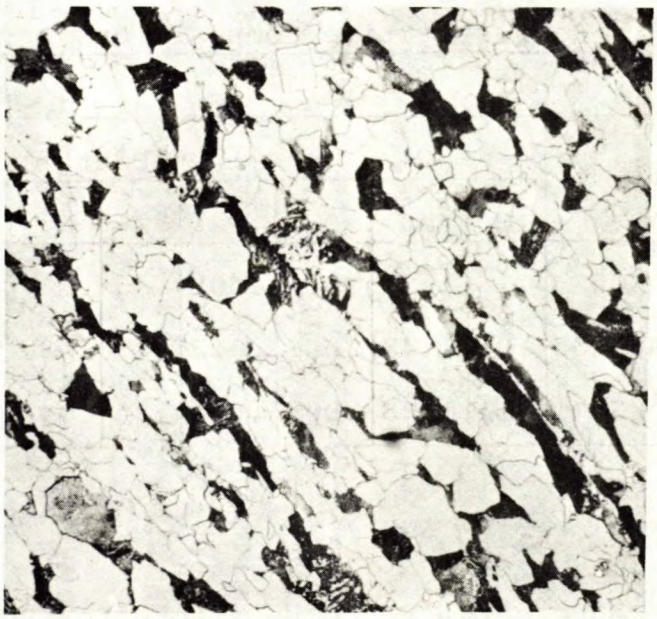

(a)

(b)

Figure 1. Optical Microstructures of Line Pipe Steels.
(a) Stelco "Grade 65", Controlled-Rolled.
(b) Ipsco "Arctic Grade 70", Controlled-Rolled. X500

TABLE 1: Representative Compositions for "Grade 65" Steels

Steel	Per Cent								
	C	Mn	S	P	Si	Nb	V	Al	Ce
Stelco X65	.16	1.25	.009	.008	.35	.047	.047		
Sumitomo X65	.05	1.43	.007	.012	.17	.028	.05		.015
Nippon X65	.11	1.28	.008	.014	.25	.04	.06	.03	

TABLE 2: Representative Compositions for "Grade 70" Steels[1,2]

Steel	Per Cent									
	C	Mn	Si	Nb	Cu	Cr	Ni	Mo	Ce	CE*
Climax Mn-Mo-Cb	.05	1.85	.15	.09				.25	.026	0.41
Molycorp X-80	.06	1.35		.10					.025	0.29
Inco 787	.05	.50		.035	1.20	.50	.85	.10		0.39

*Carbon equivalent = $\%C + \frac{\%Mn}{6} + \frac{\%Cr + \%Mo + \%V}{5} + \frac{\%Ni + \%Cu}{15}$

It should be possible to develop higher-strength steels of this type by increasing the alloy content, further modifications of the controlled-rolling practice, and additional heat treatment. However, there are several limiting factors which become increasingly important as the strength level is raised. Firstly, there is the universal inverse relation between fracture toughness and yield strength. Although this relation can apparently be reversed over a finite range of yield strengths by refining the grain size of the controlled-rolled steels (Figure 2(a)), the general trend is for the ductile-brittle transition temperature (DBTT) to

increase with increasing yield strength, (Figure 2(b)). This limits the usefulness of controlled-rolled steels for arctic-pipeline applications, since the objective is to develop a steel with higher strength and better fracture toughness than the present grade 65 and grade 70 steels. There is also a limitation due to the weldability of the higher-strength controlled-rolled steels. A "rule of thumb" indicator of a steel's weldability is the carbon-equivalent value which can be defined as $\%C + \frac{\%Mn}{6} + \frac{\%Cr + \%Mo + \%V}{5} + \frac{\%Ni + \%Cu}{15}$

When post-weld heat treatment is not possible, the carbon equivalent value should not exceed 0.40[6], and two of the three high-strength steels listed in Table 2 are up to that value already. Therefore, it will be difficult to increase the strength level of controlled-rolled steels for applications where weldability is an important consideration. Finally, the increased alloying required to achieve further increases in strength level by this means will add significantly to the cost of the finished line pipe.

It appears then that, as far as pipeline applications are concerned, the practical limits of strength of controlled-rolled steels are being approached with the recently developed Grade 70 steels[5]. Therefore, alternative types of steels and processing techniques must be considered for line pipe material that has 80 to 100-ksi (550 to 690-MN/m^2) yield strength and which is suitable for service in sections up to 1 in. (25 mm) thick in an arctic environment. Figure 2(b) indicates that the required combination of strength and toughness can be achieved only with quenched and tempered steels. This possibility is discussed further in the following section.

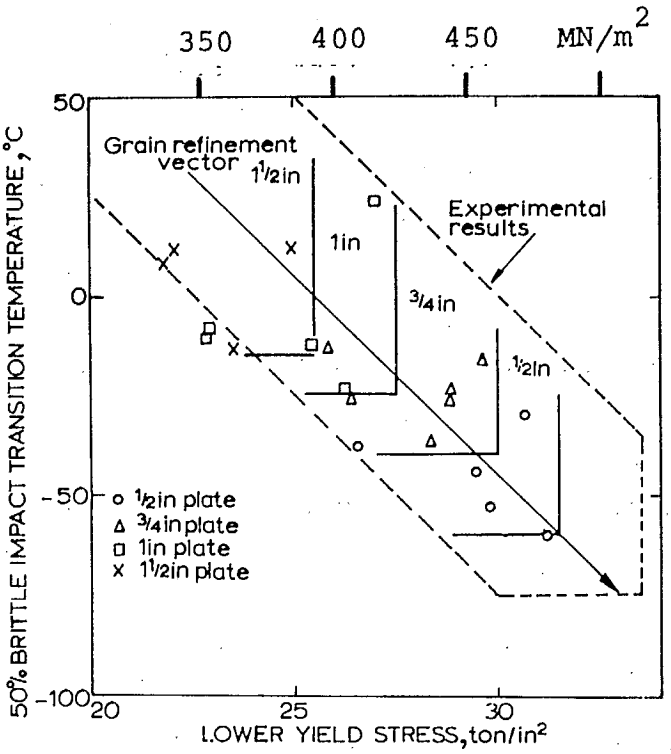

(a)

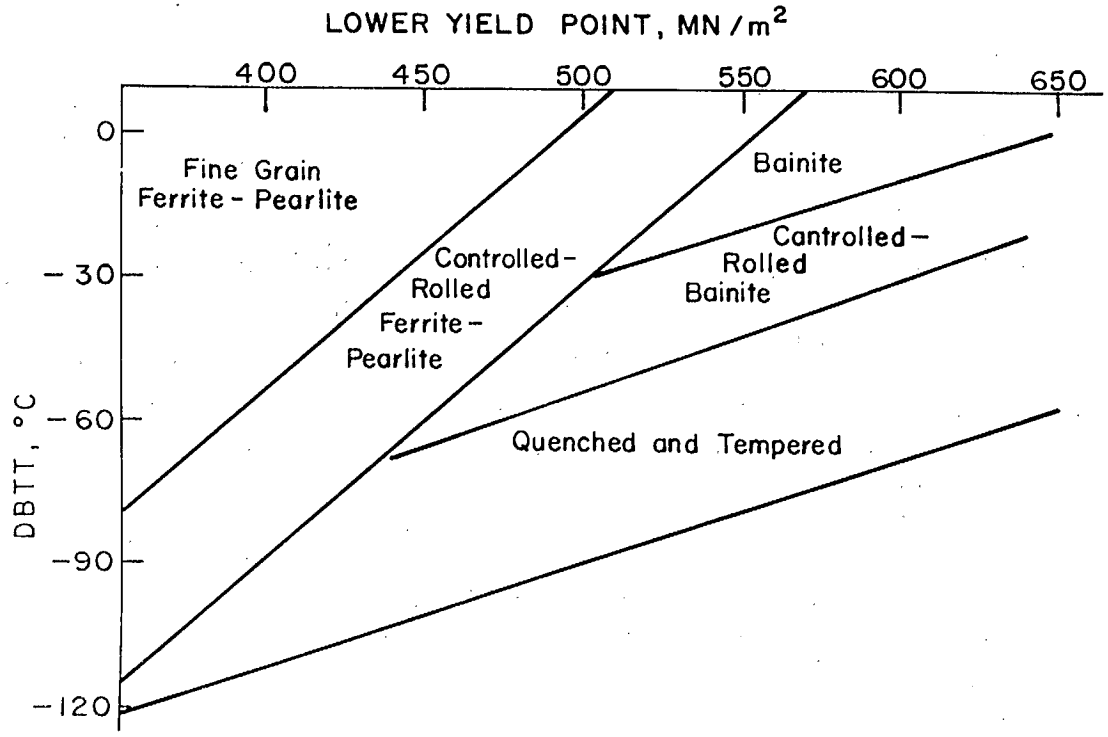

(b)

Figure 2. Relationships Between the Ductile-Brittle Transition Temperature and Yield Strength for Structural Steels (a) Controlled-Rolled 0.05C-1.5Mn-0.04Nb Steel[4]. (b) General Trends for Various Structural Steels[6].

QUENCHED AND TEMPERED LINE PIPE STEEL

Quenching and tempering can be considered to be an extension of the possible heat treatments for the existing grades of structural steels, e.g., those listed in Table 2[7]. Thus, by increasing the cooling rate from the finishing temperature (quenching) and subsequently reheating to and holding at an intermediate ageing temperature (tempering), it is possible to achieve a higher yield strength for a given alloy content than by a controlled-rolling process alone. Alternatively, the same yield strength can be obtained with a lower total alloy content. This could produce cost benefits and alleviate the weldability problem by reducing the carbon-equivalent value. The possibility of using existing grades of steel in the quenched and tempered condition also greatly simplifies the alloy development problem and minimizes the number of compositions which the commercial steelmakers have to produce[7]. However, the most important advantage of quenched and tempered steels is probably their superior toughness. Figures 2(b) and 3 illustrate that for a given yield strength the DBTT is always lower for a quenched and tempered steel than for a controlled-rolled steel. Furthermore, for a given steel its toughness in the quenched and tempered condition can be superior to that in the as-rolled condition, despite the fact that the yield strength of the former is higher, (Figure 4). The reasons why the fracture toughness of steels in the quenched and tempered condition is better than in the as-rolled or normalized condition are discussed in a later section.

It is concluded that quenched and tempered steels offer an attractive combination of strength, toughness, weldability, and economy of production for line pipe applications where 80 to 100-ksi (550 to 690-MN/m^2) yield strength is required. It has been generally recognized that quenched and tempered steels can be used advantageously as high-strength structural-steel plate products.

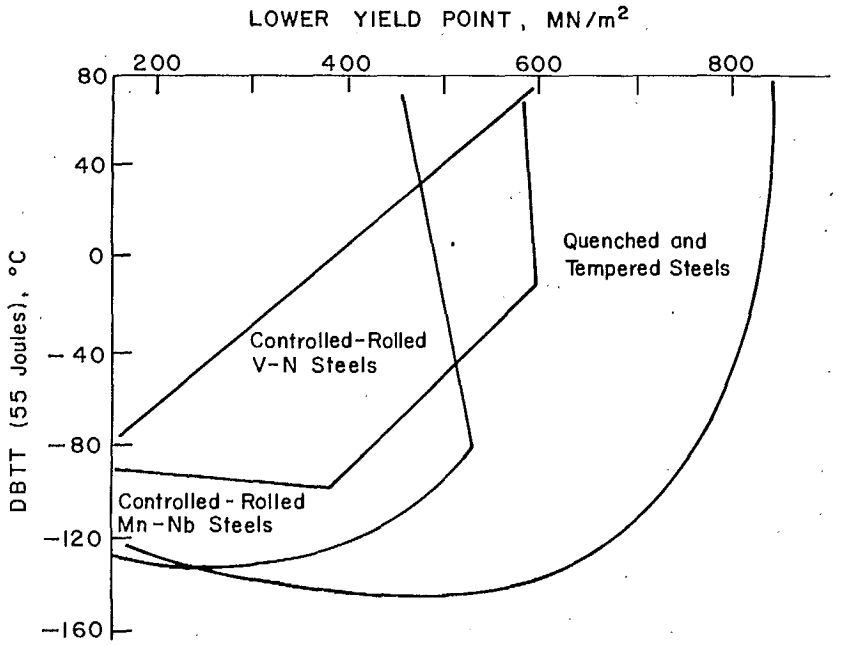

Figure 3. The Relation Between DBTT and Yield Strength for Three Types of Low-Carbon Structural Steels(5).

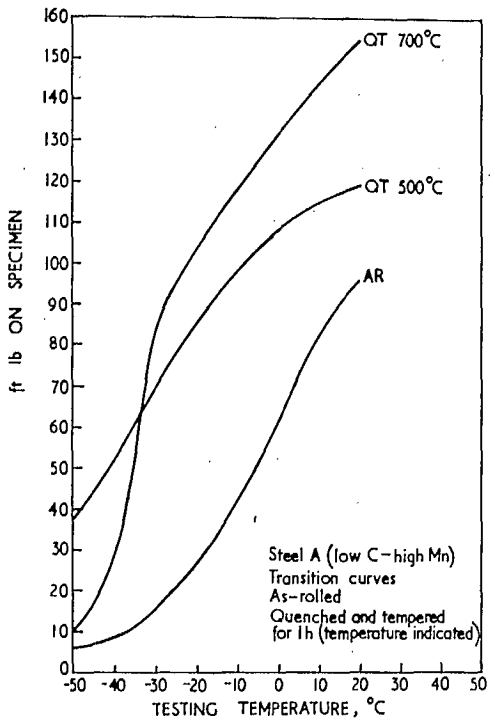

Figure 4. A Comparison of Ductile-Brittle Transition Curves for a 0.16C-1.0Mn Steel in the As-Rolled and in the Quenched and Tempered Condition(8). (55 Joules = 40.6 ft lb)

Consequently, large-scale commercial facilities have been constructed for producing quenched and tempered plate either by means of a quench press[8-10] or by a continuous roller quench[11]. Thus, considerable expertise is presently available for the production of quenched and tempered structural steel plate. However, the application of quenched and tempered steel to line pipe presents additional problems. With increasing strength level, forming and welding the pipe using quenched and tempered plate become increasingly difficult. Hence, it is necessary to consider alternative techniques for utilizing the quench and temper approach in line pipe. One possibility would be to make the pipe in the as-controlled-rolled and quenched condition, and to develop the required mechanical properties by tempering the pipe. This type of process would involve extending the present controlled-rolling techniques such that, following a direct quench, the plate can be easily formed into pipe, and the optimum microstructure can be achieved simply by tempering. A second possibility would be to make pipe from as-rolled plate, and to subject the pipe to a reheat, quench and temper treatment. It should be possible to achieve better microstructural control with this type of process, but a facility for austenitizing and quenching full-size lengths of pipe would be required. It is assumed that it is technologically feasible to produce line pipe by either of the above processes. The remainder of this report considers some of the basic metallurgical parameters relevant to both processes.

MICROSTRUCTURE OF QUENCHED AND TEMPERED STEEL

The microstructures of quenched, low-carbon steels have not been as well characterized as those of medium- or high-carbon steels. The microstructures which can occur in low-carbon steels vary widely in both type and scale, but their description is usually imprecise, and the terminology is at present very confused. Much of the difficulty arises from the use of optical microscopy alone to characterize the various structures. In many

cases the microstructural constituents are dispersed on too fine a scale to be suitably resolved optically, and structures which are quite different in type or scale have the same nondescript appearance at optical magnifications. As a result, these as-quenched microstructures have been variously identified as low-carbon martensite, pseudo-pearlite, carbon-free bainite, bainitic ferrite, blocky ferrite, Widmanstätten ferrite, acicular ferrite, and massive ferrite[1,12,23]. Each of these terms defines a particular structure fairly precisely, but they have been used interchangeably for similar structures because the distinction cannot be made by optical microscopy. However, in most cases the various structures can be differentiated by electron metallography. An attempt will be made here to use a consistent glossary of terms in order to characterize microstructures according to their final structure and to the type of transformation from the austenitic condition.

Most of the microstructures considered in this report can be initially categorized optically as either polygonal or non-polygonal ferrite. This identification indicates that the matrix is b.c.c. ferrite, and whether the ferrite grains are equiaxed (polygonal), or not, but it does not discriminate between different types of transformations. Thus, polygonal ferrite can form either by a nucleation and growth process which is diffusion controlled, or it can form by a massive transformation in which growth is controlled by a short-range transfer of iron atoms across austenite-ferrite interfaces[13]. The category of non-polygonal ferrite embraces a wide variety of structures and transformations. Figure 5 illustrates the different microstructures that can be obtained by varying the cooling rate. At the lower cooling rates, the austenite-ferrite transformation occurs by a nucleation and growth process, but the ferrite grains have an irregular shape (Figure 5(a)-(c)). At higher cooling rates, the ferrite grains become smaller and more acicular. At still higher cooling rates, the transformation product is bainite (Figure 5(d)), and at the highest cooling rates, a martensitic transformation occurs (Figure 5(e)).

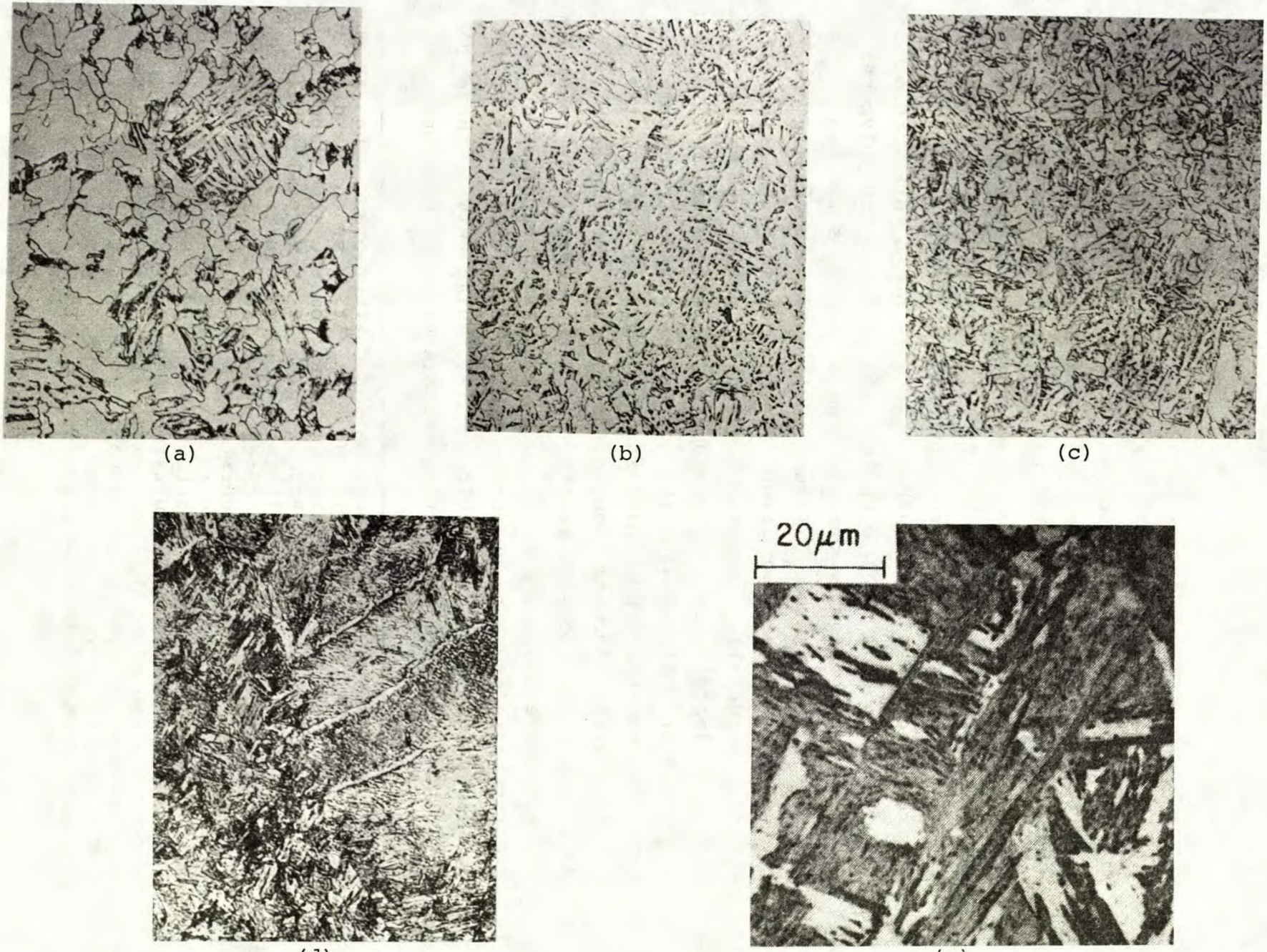

(a) (b) (c) (d) (e)

Figure 5. Variation in Microstructure with Quenching Rate for Low-Carbon Steels: (a)-(d), Fe-0.10C-1.85Mn-0.23Si-0.06Nb[16], (e) Fe-0.14C[17] (a) 1°C/S, (b) 3.5°C/S, (c) 7°C/S, (d) 50°C/S, (e) 5000°C/S.

Apart from this gross characterization, it is difficult to describe the non-polygonal ferrite microstructures any more accurately by optical microscopy. However, by using scanning electron microscopy and replica or transmission electron microscopy, it ought to be possible to determine the size and distribution of the carbides, i.e., pearlite or dispersed carbides and to identify the type of transformation*. A series of electron micrographs representing the important non-polygonal ferrite structures in low-carbon steels is shown in Figure 6. At the slowest cooling rate which still produces non-polygonal ferrite, the transformed ferrite grains contain a tangled dislocation substructure (Figure 6(a)). With increasing cooling rate, decreasing transformation temperature, and increasing alloy content, especially niobium, the ferrite grains become increasingly acicular[12], and the dislocation density goes up[1]. In this range of cooling rates the austenite-ferrite transformation probably takes place by a nucleation and growth process, the acicular ferrite forming under conditions which favor high nucleation rates and slow growth rates. However, it is possible that a massive transformation could occur which produces an acicular transformation product. Because of the rapidity of the transformation, it is difficult to distinguish between these two mechanisms. At higher quenching rates, a bainite transformation

*There is fairly good agreement on the definitions of the various types of transformations(14). However, it is sometimes difficult to identify the type of transformation from the appearance of the final microstructure. For example, it is generally held that the fundamental characteristic of a martensite or bainite transformation is the shape change which accompanies the transformation of austenite to ferrite by a shear mechanism(13). The occurrence of a shape change is conveniently indicated by surface relief effects. However, recently it has been shown that a shape change can result from a diffusion-controlled nucleation and growth transformation(15). Therefore, the appearance of the surface relief effects is not positive evidence of a shear transformation. For most purposes, however, the information obtained from electron metallography should be sufficient to identify the transformation.

can occur. That is, acicular ferrite grains form in the austenite by a shear mechanism, and the carbon segregates by diffusion to form carbides. When the carbon-diffusion rates are high enough for complete carbon segregation to the austenite, the final microstructure consists of acicular ferrite grains with a continuous network of carbide at the grain boundaries (Figure 6(b)). This is called upper bainite to distinguish it from lower bainite which forms at lower temperatures and higher cooling rates. In the latter case, complete segregation of carbon to the ferrite-austenite interface does not occur, and carbides precipitate within the ferrite grains, often associated with a tangled dislocation substructure (Figure 6(c)). At still higher quenching rates the austenite to ferrite transformation is martensitic. Two distinct types of martensite have been identified in low-carbon steels. Lath martensite consists of parallel plates or laths of ferrite which are often grouped in larger units that have a block-like appearance at low magnification[17,20,24,25] (Figure 6(d)). The individual laths contain a dislocation substructure which often consists of low-angle boundaries[21,22], and the habit plane of the laths is approximately $(\bar{2}\bar{1}3)_\alpha$[21] or $(557)_\gamma$[24]. The second type of martensite is called twinned martensite and it forms at lower temperatures than the lath martensite. Twinned martensite consists of acicular ferrite plates which have an internal structure of fine lamellar twins (Figure 6(e)).

The various transformation products that can form in low-carbon steel can be summarized on a continuous-cooling-transformation (CCT) diagram. Unfortunately, complete CCT diagrams for steels with less than 0.1C are not readily available. However, the principles can be illustrated by reference to the diagram for a 0.13C-0.56Mn steel shown in Figure 7. The cooling curves shown for 0.5-in. (1.27-cm) and 2-in. (5.08-cm) plate are for specimens reheated to and quenched from a fixed austenitizing temperature. The measured cooling rate for direct-quenched 1.3-in. (3.3-cm) plate of a 0.21C-0.85Mn steel[27] is also included in

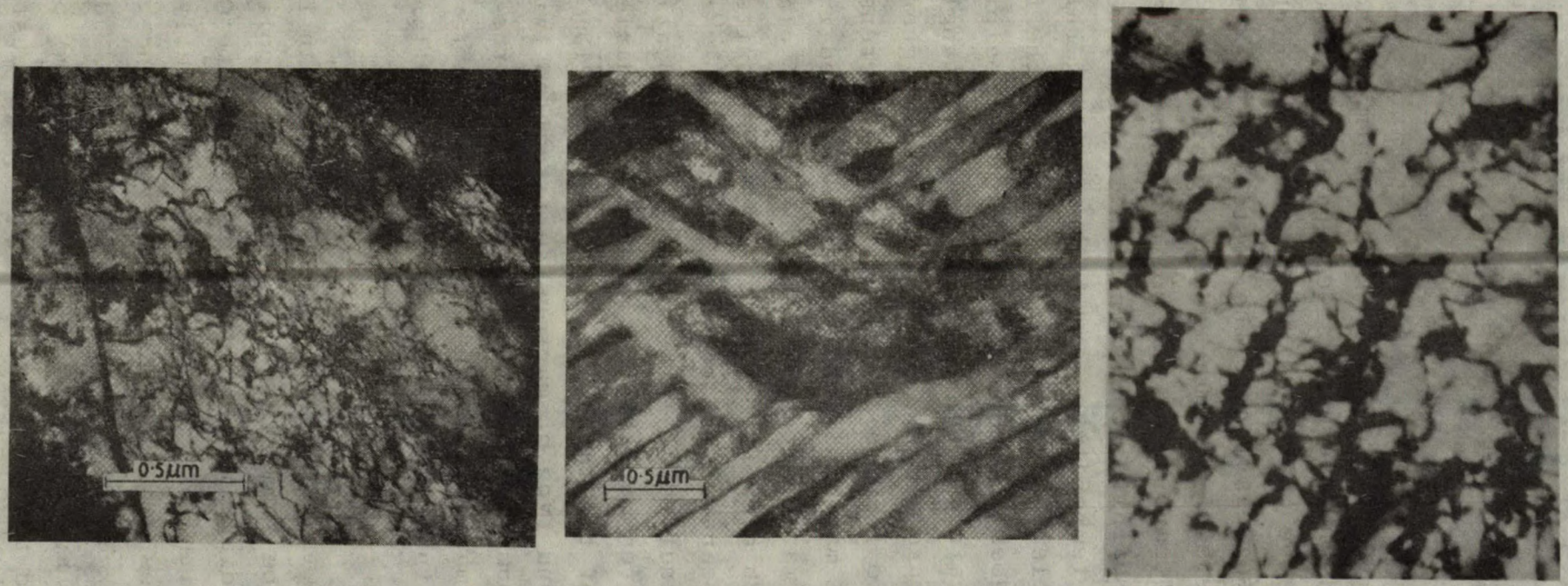

(a) (b) (c)

Figure 6. Electron Micrographs Illustrating Various Non-Polygonal Ferrite Microstructures in Low-Carbon Steels. (a) Fe-0.037C-1.42Mn-0.055Nb-.0075N. Water-Quenched from Finish Rolling Temperature of 950°C, Acicular Ferrite with Dislocation Substructure[18]; (b) Fe-0.071C-2.00Mn-0.16V-0.027N, Water-Quenched from Finish Rolling Temperature of 950°C, Upper Bainite[18]; (c) Fe-0.1C, Transformed at 450°C, Lower Bainite[58] (d) Fe-0.026C, Solution-Treated at 1000°C and Quenched at 10^4 °C/S, Lath Martensite[17]. (e) Fe-0.11C-28Ni-0.21Si, Solution Treated at 850°C and Water-Quenched, Twinned Martensite[19].

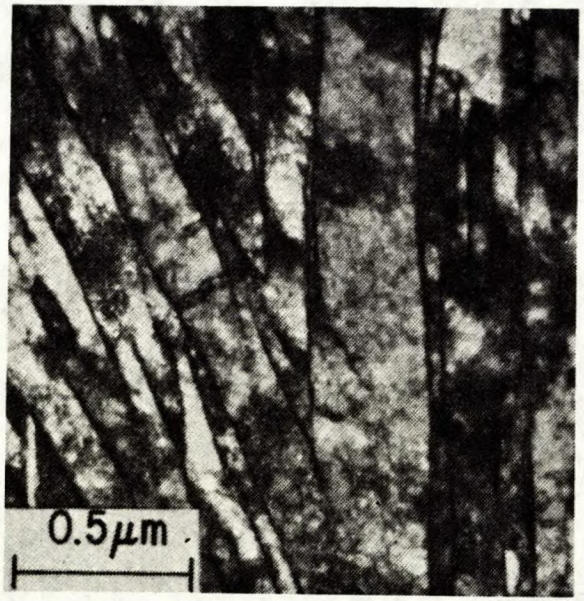

(d)

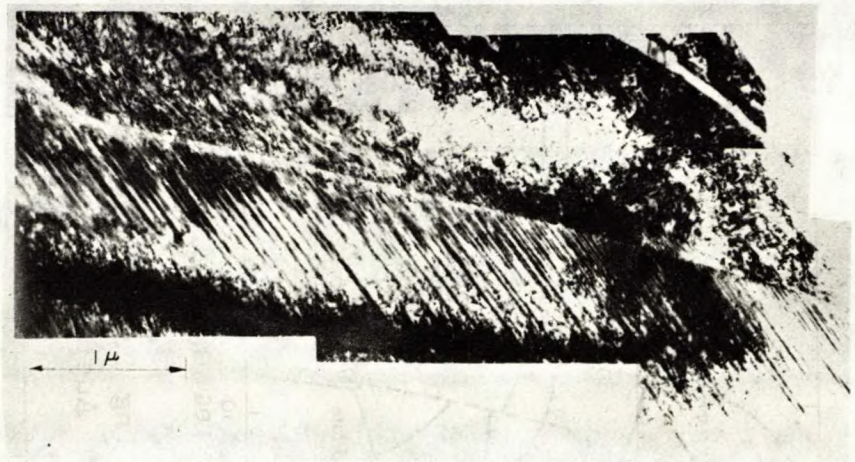

(e)

Figure 6. Electron Micrographs Illustrating Various Non-Polygonal Ferrite Microstructures in Low-Carbon Steels. (a) Fe-0.037C-1.42Mn-0.055Nb-0.0075N, Water-Quenched from Finish Rolling Temperature of 950°C, Acicular Ferrite with Dislocation Substructure[18]; (b) Fe-0.071C-2.00Mn-0.16V-0.027N, Water-Quenched from Finish Rolling Temperature of 950°C, Upper Bainite[18]; (c) Fe-0.1C, Transformed at 450°C, Lower Bainite[58] (d) Fe-0.026C, Solution Treated at 1000°C and Quenched at 10^4°C/S, Lath Martensite[17]. (e) Fe-0.11C-28Ni-0.21Si, Solution Treated at 850°C and Water-Quenched, Twinned Martensite[19].

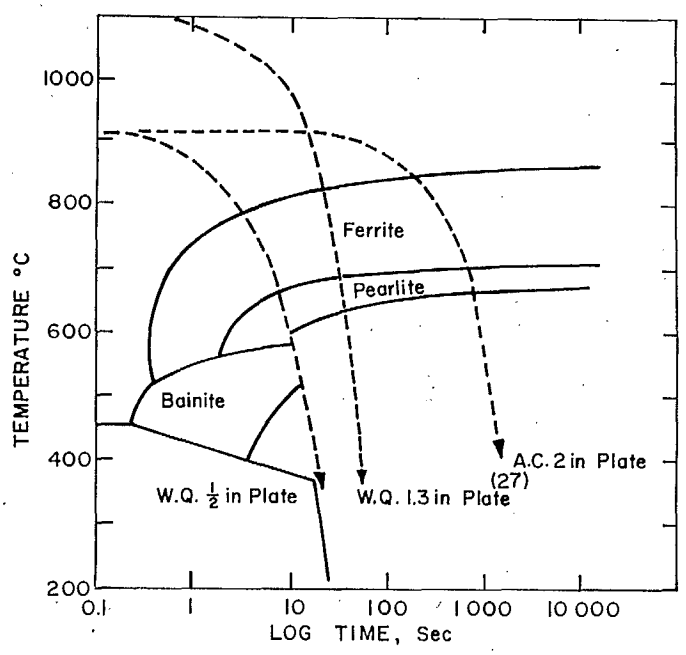

Figure 7. Continuous Cooling Transformation Diagram of Fe-0.13C-0.56Mn Austenitized at 920°C (26).

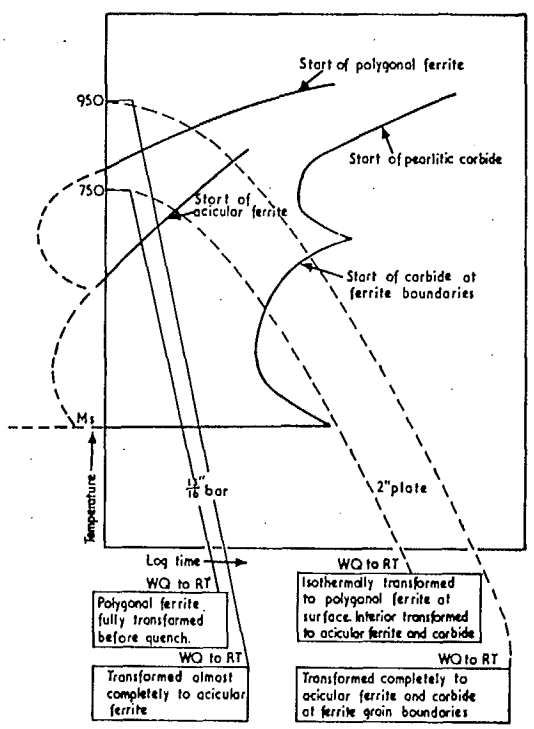

Figure 8. Schematic Representation of Continuous-Cooling-Transformation Diagram for Low-Carbon Steels(12).

Figure 7. In order to consider the effects of parameters such as alloy content, cooling rate, and austenitization temperature on the final microstructure, it is convenient to consider their effects on the temperature of the austenite-to-ferrite transformation. As the transformation temperature decreases, the final microstructure should vary from polygonal ferrite to acicular ferrite, to upper bainite, to lower bainite, to lath martensite, to twinned martensite. From this point of view, the parameters of interest determine the operative transformation temperature, and, hence, the final microstructure. For example, increasing the cooling rate decreases the transformation temperature, as shown by the cooling curves for specimens of different thickness. The same effect is achieved by adding alloy elements such as carbon, manganese, niobium, molybdenum, chromium, or nickel which tend to shift the CCT curves to the right[1]. Conversely, alloying with silicon moves the CCT curves to the left, and raises the transformation temperature for a given cooling rate.

It can be seen from Figure 7 that the expected cooling rates relevant to the manufacture of 0.5 to 1.0-in., (12.7 to 25.4-mm) thick line pipe are such that the austenite will invariably transform to ferrite + pearlite, or to ferrite + carbide. It is likely that the steel used for quenched and tempered line pipe will be of much lower carbon content than the one represented by the CCT diagram in Figure 7 and such a steel would have even lower hardenability, as shown schematically in Figure 8. Therefore, for the purpose of developing a suitable alloy and treatment for manufacturing quenched and tempered line pipe, attention can be focussed on the diffusion-controlled transformation of austenite to ferrite. The inter-relations between microstructure and the mechanical properties of quenched and tempered steels are discussed in a later section. However, it may be stated here that from the point of view of optimizing mechanical properties, the ideal transformation behaviour is represented by the cooling curve for the 13/16-in. bar in Figure 8, by which most of the austenite transforms at a low temperature to fine-grained, non-polygonal ferrite, with no precipitation of either grain-boundary carbides

or pearlite. The metallurgical parameters which control the transformation behaviour are discussed in detail below.

The parameters that are considered to be most important in determining the transformation characteristics of low-carbon steel are:

1. alloy content
2. cooling rate
3. hot-rolling schedule
4. austenitizing treatment (for a reheat-quench process).

The effects of various alloy elements on the transformation characteristics are too complex to be stated simply, but some general trends can be noted. Of the normal alloy elements, carbon has the most profound influence on the transformation behaviour but it is not relevant here because we are considering only low-carbon ($\leqslant$0.1 C) steels. The effects of other popular alloy elements on the ferrite-start temperature are illustrated in Figure 9. Manganese lowers the ferrite-start temperature significantly, (Figure 9(a)) and its use is limited only by the onset of the bainite transformation. Provided the carbon content is less than 0.4%, up to 2.0% Mn is acceptable[1,12]. Figure 9(b) shows that niobium also lowers the ferrite-start temperature, particularly in combination with other alloy elements such as molybdenum or boron. The magnitude of the effect of niobium depends on the amount of niobium dissolved in the austenite, which is in turn influenced by the carbon content and the rolling schedule[1]. This is another reason for keeping the carbon content low because the niobium solubility decreases with increasing carbon content.

The inverse relation between cooling rate and ferrite-start temperature is illustrated in Figures 8 and 9(b). This is not considered to be an important variable for controlling the microstructure of quenched and tempered line pipe because the effect is not really significant until the cooling rate is quite

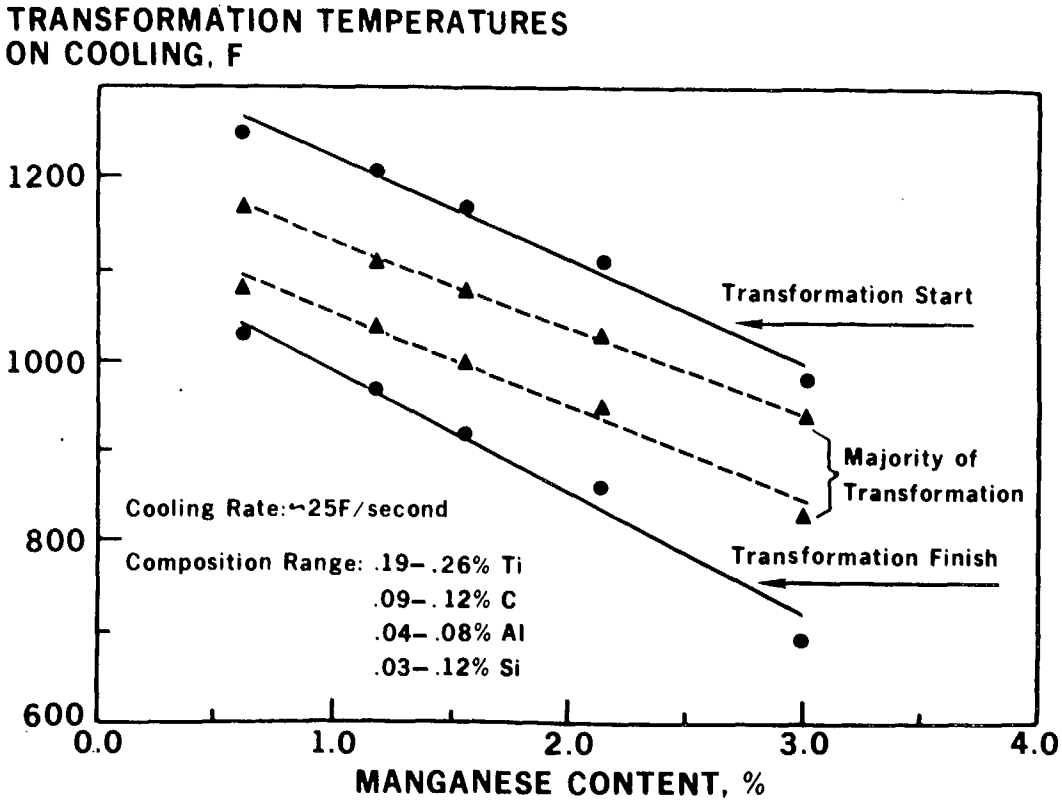

(a)

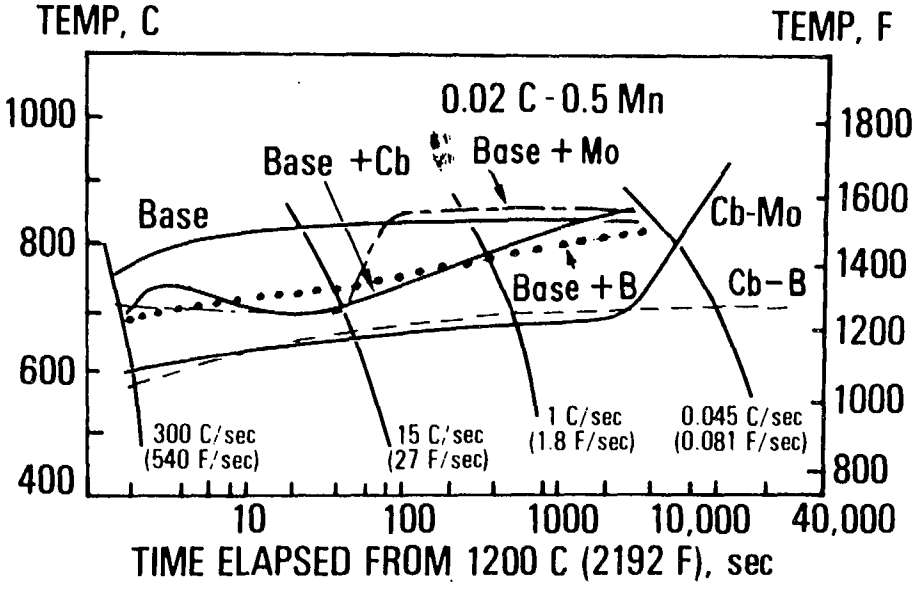

(b)

Figure 9. The Effects of Various Alloy Elements on the Transformation Temperatures in Low-Carbon Steels. (a) Effect of Manganese(1). (b) Effects of Niobium, Boron and Molybdenum(1).

high (>100°C/S); also,the cooling rate obtained in practice will probably be fixed within fairly narrow limits by the manufacturing process.

Therefore, for a given steel composition and cooling rate, the only variables that remain are the hot-rolling schedule and the austenitizing treatment (for a reheat-quench process). From the discussion up to this point, it can be appreciated that achieving the goal of a fine-grained, non-polygonal ferrite microstructure will be aided by having the smallest possible austenite grain size prior to transformation and by having such elements as manganese and niobium in solution. For a direct-quench process, the ferrite grain size is minimized by controlled rolling to a low finishing temperature and alloying with elements such as niobium, vanadium, titanium, and aluminum, which inhibits recrystallization and grain growth of the austenite[4]. Niobium seems to be the most effective element for retarding austenite recrystallization, whereas all these elements inhibit grain growth. It is believed that the specific effect of these elements on the rates of recrystallization and grain growth is the formation during the later stages of hot rolling, of a fine dispersion of carbides which pin the austenite grain boundaries and sub-boundaries. Thus, it would appear that niobium is a very useful alloy element for controlling the microstructure of low-carbon steels, but some choice must be made between the beneficial effects of niobium in solution and those of niobium-rich precipitates. Similar considerations apply for the reheat-quench process. However, it has been shown that superior microstructures and mechanical properties are obtained when a steel is quenched directly after hot rolling compared with one which is air cooled, reheated to the same finishing temperature, and quenched [12,28-30]. This phenomenon is attributed to the fact that immediately prior to direct quenching after hot rolling, the carbides are smaller and there are higher concentrations of alloying elements in solution than after the steel has been air cooled and reheated to the same temperature. However, there are no

data on the size distributions of carbides in either of these two conditions, and the exact mechanism by which the carbides inhibit austenite recrystallization and grain growth is not really understood. For either type of processing (direct quench or reheat-quench), the finishing temperature or austenitizing temperature is restricted to a range bounded by the ferrite-start temperature at the lower extreme, and by an upper extreme at which the austenite is sufficiently stabilized by dissolved alloy elements to produce bainite when quenched[12]. Within these limits, a compromise must be made between the advantages of a small grain size and high dislocation density (low finishing/austenitizing temperature) and a high concentration of alloy elements in solution which increases hardenability and aging response (high finishing/austenitizing temperature).

Finally, the microstructural changes which take place during a tempering heat treatment will be considered. Unlike the tempering of high-carbon steels, where the dominant effect is the lowering of the carbon concentration in the martensite by the precipitation of carbides, in the tempering of low-carbon steels, the most important result is the strength increase due to the precipitation of alloy carbides or nitrides (secondary hardening). The only other significant microstructural changes which could occur during tempering are segregation of carbon and rearrangement of the dislocation substructure within the ferrite grains. The tempering behaviour of low-carbon steels is illustrated by the ageing curves in Figure 10 for a 0.04C-Mn-Nb steel. The small decrease in hardness which occurs during tempering at temperatures less than 500°C is associated with the recovery of the dislocation substructure[31] and with the segretation of carbon to dislocations and sub-boundaries[32]. At the cooling rates (~10^0C/S) likely to be achieved in quenching line pipe steel, there will be considerable segregation of carbon to dislocations during the quench, (it has been shown that segregation occurs at cooling rates as high as 10^4°C/S provided that the carbon content is less than 0.2%[32]). In plain carbon steels,

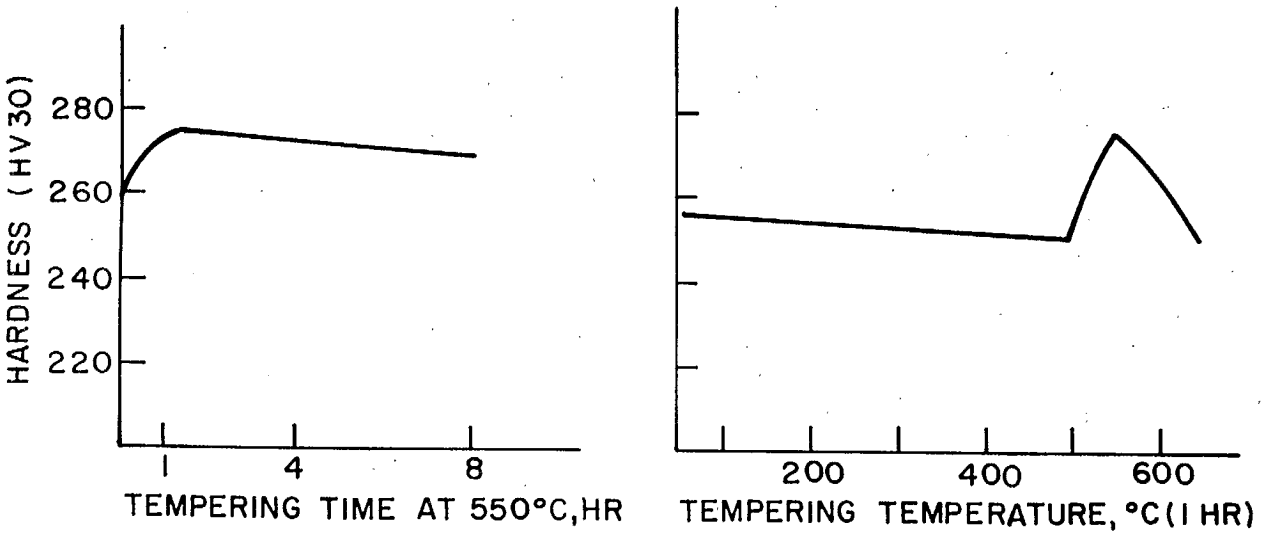

Figure 10. Precipitation Hardening Behaviour for Fe-0.04C-2.10Mn-.11Nb Controlled-Rolled and Water-Quenched from a Finishing Temperature of 950°C(18).

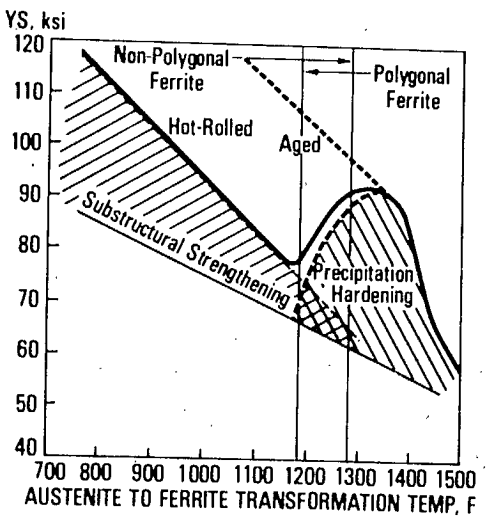

Figure 11. Relative Effects of Various Strengthening Mechanisms for Controlled-Rolled Plate(1).

rod-shaped carbide precipitates have been detected after tempering at temperatures between 150°C and 350°C[32-34]. The exact nature of this carbide phase is not known, but diffraction evidence has been found for ε-carbide[35], Hägg carbide[36], and cementite (Fe_3C)[34]. However, in steels containing alloy additions of manganese, niobium, vanadium, etc., there is no apparent carbide precipitation at tempering temperatures below 500°C[12,18]. The secondary hardness peak which occurs upon tempering low-carbon, low-alloy steel between 500 and 650°C (Figure 10) is attributed to the precipitation of alloy carbides, nitrides, or carbonitrides[12,18]. These precipitates nucleate preferentially on the dislocation substructure in the ferrite grains. The precipitate phase is thought to be NbC in niobium-containing steels, but the precipitate structures have not been determined for either the vanadium-nitrogen or the niobium-nitrogen steels. In copper-containing steels, the precipitate phase is either ε-copper[1] or elemental copper[12]. For the plain carbon steels, the ferrite grains recrystallize when tempered at temperatures above 500°C[32], whereas, in the low-carbon low-alloy steels the carbide precipitates stabilize the dislocation substructure for tempering temperatures up to approximately 650°C[12]. Therefore, it should be possible to select an ageing treatment which gives the combination of precipitation hardening and substructural strengthening consistent with optimum mechanical properties. It appears that the precipitation kinetics depend strongly on the character of the dislocation substructure in the as-quenched ferrite grains. An indication of this is the fact that niobium carbide precipitates form at lower tempering temperatures in the presence of a dislocation substructure than in dislocation-free material[18]. The possibility of controlling the final distribution of precipitates by varying the dislocation substructure has not yet been investigated systematically.

MECHANICAL PROPERTIES OF QUENCHED AND TEMPERED STEELS

Having discussed the various ways of controlling the microstructure of quenched and tempered steels, we now consider the relations between microstructure and some of the important mechanical properties. As usual, the alloy selection or development problem is essentially one of obtaining the best combination of yield strength and fracture toughness. Therefore, most of the discussion deals with these two properties. However, other mechanical properties such as formability, weldability, and susceptibility to stress-corrosion cracking are also important, and these are considered briefly at the end of this section.

Strengthening Mechanisms

The important methods of strengthening quenched and tempered low-carbon steel are:

1. grain-size control
2. dislocation-substructural strengthening
3. precipitation hardening
4. solid-solution strengthening

The lower yield stress varies inversely with the square root of the grain size according to the well-known Petch relation[37]. Theoretically, this relation follows from the fact that the shear stress in an undeformed grain at a distance r from a grain containing a dislocation pile-up of length d is

$$\tau = (\tau_y - \tau_i)\ (d/r)^{1/2} \qquad (1)$$

where τ_y is the applied shear stress, and τ_i is the effective shear stress in a slip band. Hence, the lower yield stress for a polycrystalline specimen is given by the Petch equation

$$\sigma_y = \sigma_i + kd^{-1/2} \qquad (2)$$

Practically, the Petch relation indicates that the lower yield stress can be increased indefinitely by refining the grain size, the strength increment varying with the value of the parameter k. It is not clear how the grain morphology affects yield strength. The high yield strengths which are found for the acicular ferrite grain morphology can probably be attributed to the small effective grain size rather than to any effect of grain shape per se.

The magnitude of the dislocation-substructural strengthening effect is illustrated schematically in Figure 11 for controlled-rolled plate. Apparently the yield strength varies directly with the dislocation density which is determined largely by the austenite-to-ferrite transformation temperature. Comparing the load-extension curves for a low-carbon steel in the as-quenched and in the quenched and tempered conditions (Figure 12) indicates that the dislocation substructure influences the yielding and work-hardening behaviour[12,33] in addition to contributing to the yield strength. The load-extension curve for a specimen in the as-quenched condition exhibits continuous yielding and work hardening with no obvious yield point. By contrast, the curve for a quenched and tempered specimen exhibits a sharp yield point and a very low work-hardening rate. This behaviour is attributed to the fact that, in the as-quenched condition, the mobile dislocation density is high and the dislocation substructure provides the dominant intragranular obstacles to the movement of glide dislocations. However, the precipitates which form during tempering pin the dislocation substructure and drastically reduce the mobile dislocation density. Therefore, when the stress required to overcome the precipitate obstacles is reached, there is a rapid increase in the density of mobile dislocations, and a "yield drop" occurs in a constant-strain-rate test according to

the relation

$$\dot{\epsilon} = \rho \, \underline{b} \, v \qquad (3)$$

where $\dot{\epsilon}$ = strain rate,

ρ = mobile dislocation density,

$\underline{b}$ = Burgers vector of the glide dislocations, and

v = dislocation velocity which is, in turn, a function of stress.

Furthermore, in the quenched and tempered condition, the precipitates are the dominant obstacles to the movement of glide dislocations, and the pre-existing dislocation substructure is not so important. The low rate of work hardening suggests that, once a slip band has penetrated a grain, it is easier for slip to concentrate there rather than in an undeformed region. This could be explained by the mechanism proposed by Gleiter and Hornbogen[38] provided the carbide and nitride precipitates are sheared by the glide dislocations, as suggested by Nicholson[39].

The magnitude of the strength increment due to precipitation reactions is indicated by the broken line in Figure 11. It has been established that the strength increment varies with the size and volume fraction of the precipitate particles (Figure 13), in agreement with the theories of precipitation hardening[39]. The alloy elements (Nb, V, Zr, Ti) which are conventionally used to promote precipitation hardening have been selected because they tend to form precipitates in the size range which gives maximum strengthening ($<100\text{Å}$). However, there has not been a systematic study of the relation between the size distribution of the various precipitate phases and the resulting yield strength. As mentioned previously, by suitable quench and temper treatments it ought to be possible to control the precipitate size distribution and dislocation substructure to optimize strength and toughness.

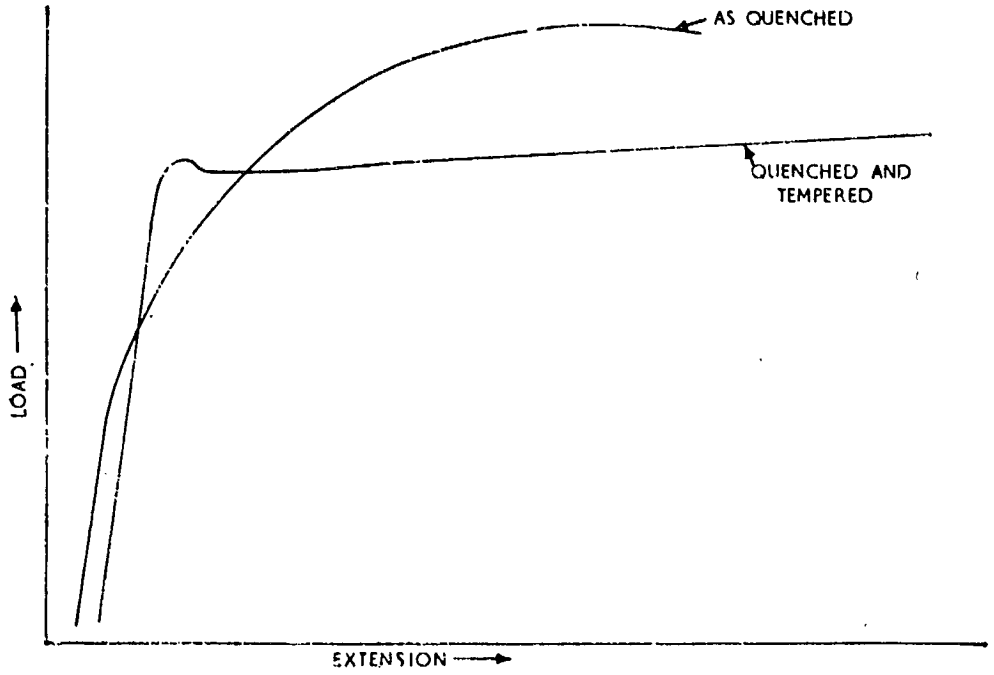

Figure 12. Typical Load-Extension Curves for an As-Quenched and Quenched and Tempered Low-Carbon Steel(12).

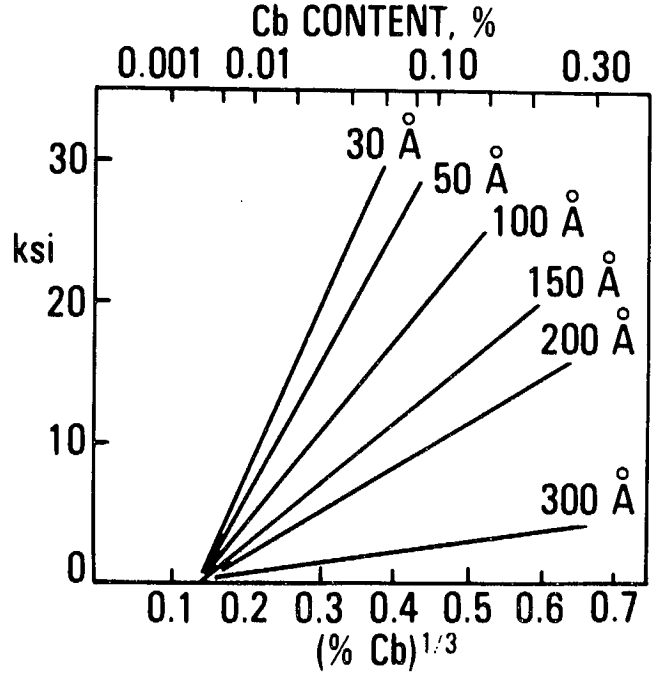

Figure 13. Effects of Volume Fraction and Precipitate Size on the Strength Increment Due to NbC Precipitation in Controlled-Rolled Plate(1).

Compared with the other mechanisms discussed here, solid-solution strengthening is not a very efficient or flexible method of achieving high yield strengths. It is well known that elements such as carbon, nitrogen, phosphorus, tin, and antimony produce the largest increments in yield strength per weight of alloy. However, all of these elements have serious adverse effects on other mechanical properties which prevent their being used extensively for solid-solution strengthening. Only the elements manganese and nickel can be used in significant amounts for their solution-strengthening effects, because they simultaneously increase toughness and yield strength. Both of these elements produce grain refinement, but the effects on toughness and strength are greater than those expected from grain refinement alone. The beneficial effect of manganese is greatest in alloys which contain large grain-boundary carbides, because the specific effect of manganese is to refine the carbide size[40]. This mechanism is probably not relevant to quenched and tempered low-carbon steels but, as stated previously, it is worthwhile to alloy with up to 2.0% Mn for purposes of grain refinement and hardenability. Nickel, on the other hand, directly influences the plastic deformation behaviour of the ferrite matrix. Specifically, it has been shown that nickel in solid solution promotes cross slip in ferrite down to temperatures as low as 50°K[41], this correlates with a decreased DBTT and an increased Charpy shelf energy. Unfortunately, the amount (>1.0%) of nickel required to realize this beneficial effect makes it a rather uneconomical alloy addition.

To summarize, it appears that significant strengthening effects can be achieved in quenched and tempered low-carbon steel by means of grain refinement, precipitation hardening, and dislocation-substructural strengthening. From the experience with controlled-rolled steels, the methods of grain-size control are well understood. The principles of precipitation hardening and substructural strengthening are also known, but there is a need to investigate the conditions of quenching and tempering which

produce the ideal microstructure. The essential problem is to identify the metallurgical condition which provides the optimum combination of yield strength and other mechanical properties, notably fracture toughness.

Fracture Toughness

The objective of all fracture toughness testing is to determine a material's behaviour in the presence of cracks or flaws for different structural configurations. In its simplest form, the criterion for crack extension is[42]

$$G \geq G_c = R \qquad (4)$$

where G is the energy per unit area provided by the loaded structure, (strain energy change plus external work), during an incremental extension of the crack, and R is the energy absorbed by the material in the process of crack extension. G is called the strain energy release rate, and R is the material's resistance to crack extension or, more commonly, its fracture toughness. A proper evaluation of the fracture behaviour of an engineering structure involves two disciplines; applied mechanics which is concerned with evaluating G for different loading geometries, and materials science which is concerned with determining R for different materials. In this report we are mainly concerned with the effects of metallurgical variables on R for line pipe steels. However, the mechanics of the fracture of a pipeline must be considered briefly in order to decide what type of fracture-toughness test is most suitable for the problem at hand.

From the point of view of crack propagation, gas pipelines are unstable engineering structures. In other words, once a crack has started to move, the loading is such that it will continue to propagate, (provided the crack velocity is sufficiently high that the structure is not unloaded by axial decompression). Examinations of service failures and full-scale burst tests[43,44] have established that the normal mode of failure is by rapid,

unstable shear-crack propagation. The crack speed is typically 400 to 800 ft/sec (122 to 244 m/sec) for X65 grades, and 800 to 1200 ft/sec (244 to 366 m/sec) for higher-strength grades. Therefore, in order to evaluate a material's resistance to this type of crack propagation, it is necessary to employ a test which effectively simulates the conditions of rapid, unstable shear crack propagation which occur in actual pipelines. Thus, the ideal test geometry would be one of convenient scale in which an unstable shear crack could be propagated at the appropriate velocities, and the corresponding energy absorption measured, preferably as a function of crack speed. The importance of such a dynamic toughness test lies in the possibility that R is sensitive to crack speed. That is, under conditions of unstable crack growth the effective value of R could be different from that measured by breaking a specimen containing a static crack. At present, most of the data on fracture toughness of line pipe steels are reported as DBTT, Charpy V-notch energy at a specific temperature, Charpy shelf energy, or the equivalent values measured in a drop-weight tear test (DWTT). None of these methods is entirely satisfactory for measuring dynamic toughness, principally because they fail to distinguish between the energy required to initiate the unstable crack and the energy for propagation. Instrumented Charpy tests indicate that the proportion of the total impact energy which is absorbed in propagation varies from zero at the low-toughness end of the transition curve to approximately 2/3 at the high end (the "shelf")[45]. Thus, it could be misleading to compare impact energies of different steels at different points on the transition curve. For comparing different steels and/or metallurgical conditions, the most reliable toughness parameter for line pipe steels is probably the shelf energy measured in a drop-weight, or pendulum-impact, tear test.

Although the mechanism of shear crack propagation is not understood in detail, the process can be described simply as two sequential events. First, an array of voids forms in the plastic zone ahead of a stressed crack and, subsequently, the voids link up leading to extend the crack. This process produces a fracture which has a"fibrous" appearance at low magnifications, and the characteristic "dimpled" appearance at high magnifications[42]. The critical strain (smooth specimen) or the critical crack-opening displacement (notched specimen) at which fracture occurs is the strain at which the voids begin to link up. It is possible for the voids to form continuously with increasing strain and to remain stable, but once they begin to link up, crack extension and fracture occur immediately[46,50]. In order to evaluate the effects of various metallurgical parameters on fracture toughness it is convenient to consider the two stages of the fracture mechanism separately.

The nucleation of internal voids is usually controlled by the distribution and type of second-phase particles. Weakly bonded brittle particles will fracture or decohere from the matrix at low stresses and strains to form an array of holes whose size and spacing are approximately equal to those of the particles. Non-metallic inclusions in steel fall in this category. More strongly bonded brittle particles require higher stresses to nucleate internal voids. Particles in this category tend to be 0.1 to 1μm in size, an example being cementite in steel in the form of pearlite, spherodite, bainite, or grain-boundary carbide. Very strongly bonded tough particles do not fracture or decohere easily and in this case, (and in the absence of any second-phase particles), the voids often form where slip bands intersect obstacles such as grain boundaries or other slip bands.

For steel, the nucleation sites of the internal voids vary with the strength level. At low yield strengths ($\sigma_y \leq 80$ ksi, 550 MN/m^2), the non-metallic inclusions are the important void-nucleation sites. These particles, which are

present in all commercial steels are extremely weak and form an array of internal voids at very low strains. Often, structural members will have a pre-existing array of internal voids resulting from fracture of the inclusions during fabrication. The fracture toughness of such steels can be increased by decreasing the volume fraction of such inclusions, or by making them more equiaxed, (Figure 14). For steels having higher strengths (σ_y = 100 to 150 ksi, 690 to 1030 MN/m^2) the cementite particles appear to be the important void formers. Of course, voids also form at the nonmetallic inclusions, but it is the fractured carbides which link up and cause crack extension[46]. Once again, the fracture toughness is controlled by the volume fraction, distribution, and morphology of the carbide particles. If it is not feasible to reduce the volume fraction by lowering the carbon content, a considerable improvement in toughness, can be realized by controlling the distribution and shape of the carbides. A fine, homogeneous distribution of equiaxed carbides is best[47]. Therefore, pearlite, bainite, and carbides on grain boundaries or subboundaries are to be avoided. By this standard, the microstructures which can be obtained in quenched and tempered low-carbon steel should produce superior toughness. The effects of volume fraction and type of second-phase particles on the toughness of steel are summarized by the data in Figure 15.

The character of slip in the matrix also influences the formation of voids at second-phase particles. The local strain in a slip band, ϵ^* is given by

$$\epsilon^* = \bar{\epsilon} \frac{d}{w} \qquad (5)$$

where $\bar{\epsilon}$ is the average macroscopic strain, d is the slip-band spacing and w is the width of the slip bands, (Figure 16). Because the maximum shear stress at the interface of a non-deforming particle is a function of the local strain in the impinging slip

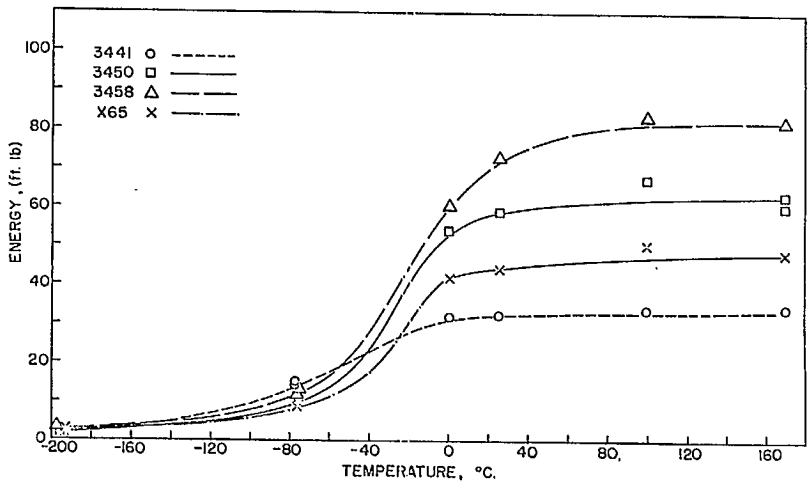

Figure 14. Charpy Impact Energy Transition Curves for Four Low-Carbon Structural Steels[46].
(a) 0.09C-2.0Mn-0.047Nb-0.15Si-0.013P-0.016S-0.118Al (3441),
(b) 0.13C-1.64Mn-0.25Si-0.013P-0.006S-0.03Al (3450),
(c) 0.19C-1.65Mn-0.06Nb-0.34Si-0.017P-0.003S-0.05Al (3458),
(d) 0.11C-1.34Mn-0.021Nb-0.32Si-0.013P-0.015S-0.04Al (X65).

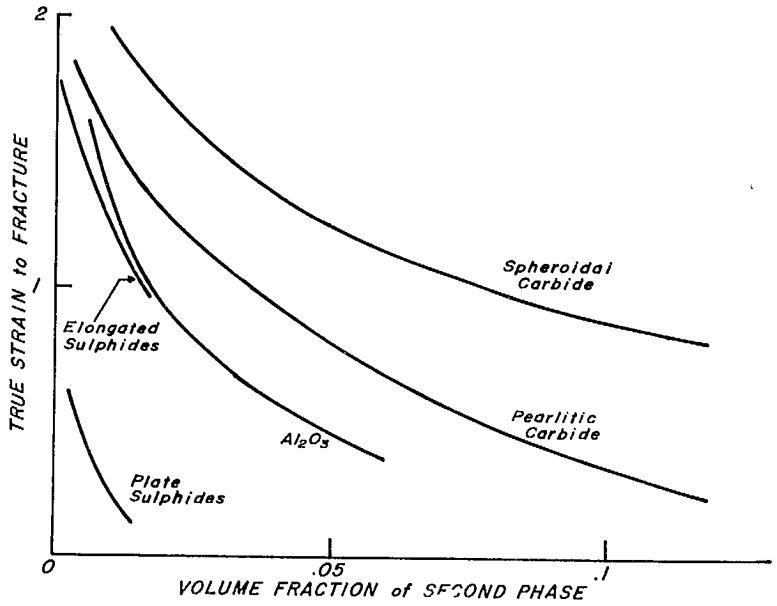

Figure 15. An Illustration of the Relation Between Second-Phase Particles and Fracture Toughness[47,50].

band[48],

$$\tau_{max} \simeq Gf\epsilon^* \qquad (6)$$

where G is the matrix shear modulus, and f is the volume fraction of particles, the stresses and strains at the particle interfaces are higher for a non-homogeneous slip character. That is, other things being equal, for a given average macroscopic strain, the number of voids at particles should increase with the ratio d/w. In this way the basic slip mechanism in the ferrite matrix can affect the distribution of internal voids and, hence, the fracture toughness. Unfortunately, it is difficult to arbitrarily control the slip character without affecting other properties, notably yield strength. However, it is a factor to be considered in alloy development.

It can also be rationalized that the well-known inverse relationship between grain size and fracture toughness is due in part to an effect of grain size on the void-nucleation process. Equation (6) refers to the stress due to the "geometrically-necessary" dislocations which form at the interface of a non-deforming particle to maintain compatibility, as illustrated by the lower particle in Figure 16. In addition, a particle can experience a stress due to a pile-up of glide dislocations in the impinging slip band. The magnitude of this contribution to the stress is a function of the length of the pile-up and, thus, is limited by the grain size[47]. The little experimental data available indicate that the effect of grain size on toughness is small compared with the effect of second-phase particles[49]. However, with increasing strength level the relative importance of second-phase particles decreases. For the highest-strength steels (σ_y >200 ksi, 1380 MN/m^2), it appears that slip is extremely non-homogeneous and that the internal voids nucleate directly at the slip bands[51].

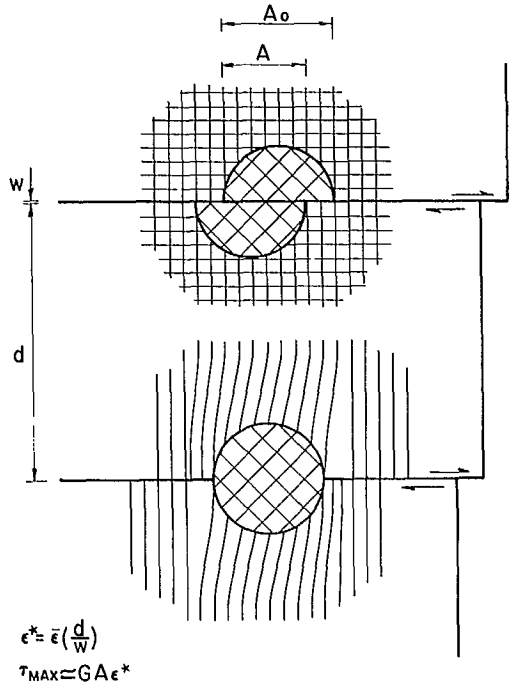

Figure 16. A Schematic Illustration of the Lattice Displacements Associated with Deformable and Nondeformable Particles. w = Slip-Band Width, d = Slip-Band Spacing.

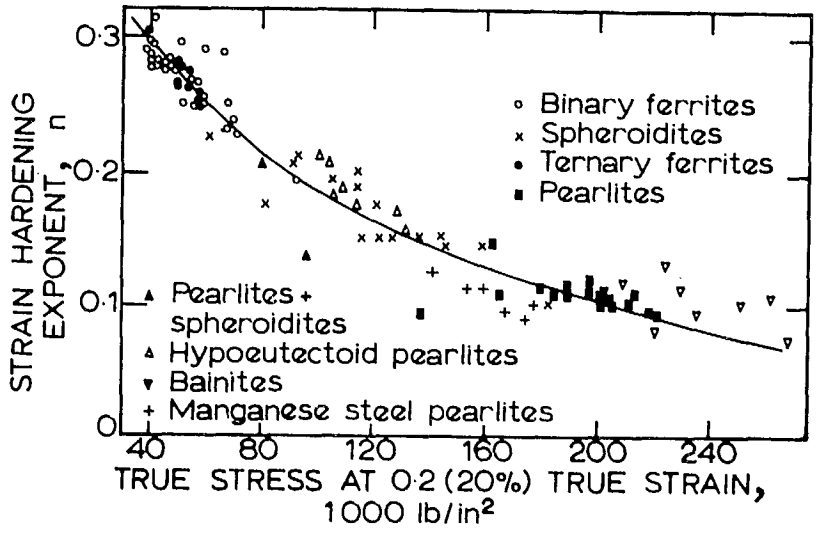

Figure 17. The Variation in Strain-Hardening Exponent with Strength Level for Structural Steels(56).

The process of void growth and coalescence at a crack tip has not been treated rigorously[42]. No theoretical model exists which can predict the strain or crack-opening displacement at which void coalescence begins. However, some qualitative features of the process are reasonably well established. From the above discussion of the void-nucleation process it is apparent that the most closely spaced voids are the ones which will link up. The simplest model predicts that link up will take place when the average strain is equal to $\lambda/2r$, where λ is the centre-to-centre spacing of the voids, and r is the particle radius. For randomly distributed spherical particles this reduces to a simple relation between fracture strain and the volume fraction of second-phase particles which have voids associated with them,

$$\epsilon_f = 0.64\ f^{-1/3} \qquad (7)$$

Equation (7) correctly predicts some of the important effects of microstructure on fracture toughness. Other things being equal, the fracture toughness should decrease as the volume fraction of cracked or decohered particles increases. This is in agreement with the well-established fact that the toughness of structural steel varies inversely with the inclusion content. Because the volume fraction of voids at a given strain tends to increase with increasing yield strength, there should also be an inverse relation between yield strength and fracture toughness. This is also a well-established fact but, to the author's knowledge, it has not been previously rationalized in this way using the simple void-coalescence model. Equation (7) is limited by the fact that it assumes a homogeneous strain throughout the crack-tip plastic zone without taking into account localized strain due to state of stress or micro-deformation mechanisms. As deformation becomes increasingly non-homogeneous the critical strain for void coalescence can be achieved at progressively lower average macroscopic strains, according to Equation (5). Therefore, factors which prevent highly localized strain, such as high rates of work hardening and a homogeneous slip character should improve fracture

toughness. At low deformation rates ($\dot{\epsilon} \sim 0.1\ min^{-1}$), iron and mild steel have low rates of work hardening[46] and an extremely non-homogeneous slip character[52]. However, it is the properties at much higher strain rates that are relevant to dynamic toughness. Here, the situation is very confused. It appears that for b.c.c. crystals the rate of work hardening decreases and slip also becomes more homogeneous as the strain rate is increased[53]. Introducing obstacles such as non-deformable particles, which should make slip more homogeneous may also increase the volume fraction of voids and end up being counter-productive. The significance of the dislocation substructure is equally unclear. For unrecovered, tangled,dislocation substructures there is generally a decrease in toughness with increasing dislocation density. However, this trend can be reversed by introducing sufficient cold work and employing a suitable annealing treatment to form a recovered substructure with a small subgrain size[54]. The aforementioned effect of nickel as an alloy addition is also relevant in this respect. Nickel apparently makes slip more homogeneous by promoting cross slip and this is accompanied by a significant increase in toughness[40,41]. Obviously, it is impossible to make any quantitative predictions about the specific influence of these various microstructural parameters on fracture toughness. The general trend which is difficult to escape is the decrease in toughness with increasing yield strength. This trend can also be rationalized by the void coalescence mechanism in that a decreased rate of work hardening and, hence, increasingly localized deformation usually accompany increases in yield strength[42] (Figure 17).

Despite the uncertainty about the details of the mechanism of shear-crack propagation, some qualitative statements can be made about the fracture toughness of quenched and tempered line-pipe steel. The volume fraction of internal voids, for a given strain, can be reduced by

1. reducing the inclusion content
2. making the inclusions more equiaxed
3. reducing the carbon content
4. ensuring that the second-phase transformation products are homogeneously distributed and equiaxed
5. refining the ferrite grain size

Obviously, there are practical limits to the extent to which any of these methods can be employed. It appears that, for quenched and tempered low-carbon steel having yield strengths up to 100 ksi (690 MN/m^2), the volume fraction and distribution of the transformation products are such that they do not contribute significantly to the volume fraction of internal voids, f_v, during straining. Therefore, f_v is determined largely by the amount, shape, and type of non-metallic inclusions, and these parameters should be controlled to the limit of practicability. Refining the ferrite grain size is also an efficient way of limiting f_v. Given the best relation between f_v and strain that can be obtained, the strain at which the voids link up and, hence, the fracture toughness, is determined by the plastic deformation behaviour of the ferrite matrix. A considerable research effort is required to clarify the effects of the various metallurgical parameters on the void coalescence process, and to synthesize the microstructure with the optimum combination of strength and toughness. At present, it appears that alloying with nickel is definitely beneficial, although the cost may be prohibitive for line pipe steel. The slip character in quenched and tempered steels is more homogeneous than in pearlitic steels[55], which is encouraging. However, on a macroscopic scale, the work hardening rate of quenched and tempered steel is still very low (Figure 12).

Formability, Weldability and
Stress-Corrosion Susceptibility

Because good formability is essentially a matter of avoiding localized strain and fracture during the forming operation, the same considerations apply as for ductile fracture. This subject has recently been discussed by Wilson[56]. For the specific problem of forming line pipe it is germane to note that the presently existing pipe-forming equipment could be used for the higher-strength quenched and tempered steels. This is due to the fact that the pipe would be formed before the final strength is achieved by heat treatment.

The critical welding operation for quenched and tempered line pipe will be the circumferential weld which will be made in the field. For the purpose of alloy development, the aforementioned rule of thumb that the carbon-equivalent value should be less than 0.40 is as good a criterion as any. By this standard the low-carbon steels that are envisaged for quenched and tempered line pipe should be quite satisfactory. However, it will be necessary to perform extensive tests of the weldments.

The stress-corrosion cracking of line-pipe steel has recently been reviewed by Biefer[57]. It would appear that this type of failure should not be a significant problem for the yield strengths and operating conditions which are anticipated for a northern pipeline.

SUMMARY AND CONCLUSIONS

The practical limits of strength of controlled-rolled line pipe steels are being approached with the recently developed Grade 70 steels. It appears that alternative types of steels and processing techniques must be considered for higher-strength line pipe material. For large-diameter, heavy-walled line pipe in which 80 to 100-ksi(550 to 690-MN/m^2) yield strength is required, quenched and tempered low-carbon steels (<0.1 C) offer an attractive combination of strength, toughness, formability, weldability, and economy of production. The combined effects of an extremely fine ferrite grain size, a dispersion of alloy carbonitride precipitates, and a dislocation substructure make it possible to achieve a higher yield strength per alloy content with a quench and temper treatment than by controlled rolling alone.

Line pipe could be produced in the quenched and tempered condition by either of two methods:

1. make the pipe from as-controlled-rolled-and-quenched plate, and develop the required mechanical properties by tempering the pipe;
2. make the pipe from as-rolled plate, and subject the pipe to a reheat-quench and temper treatment.

Some generalizations can be made about the control of microstructure and the relation between microstructure and mechanical properties for this type of steel, but commercial production of line pipe by either of these two methods would require extensive developmental research to delineate the processing conditions which produce the optimum combination of mechanical properties.

The final microstructure of quenched and tempered low-carbon steel can be controlled by varying the alloy content, hot-rolling schedule, cooling rate, austenitizing treatment (for the reheat-quench-temper process), and tempering treatment. The general procedure is:

1. minimize the austenite grain size by alloying with niobium, vanadium, aluminum, or titanium and by controlling the rolling schedule;
2. ensure that the austenite transforms to a fine-grained ferrite by alloying with niobium and manganese to lower the transformation temperature, by having a low finishing temperature (or a low austenitizing temperature for a reheat-quench process), and by having a fast cooling rate; any carbides present in the as-quenched condition should be homogeneously-distributed intragranular precipitates rather than pearlitic, bainitic or grain-boundary carbides;
3. develop the required distribution of alloy carbides or carbonitrides by a suitable tempering treatment.

The required yield strength is obtained by the combined effects of the fine grain size, dislocation substructural strengthening, and precipitation hardening. Solid-solution strengthening is not an important strengthening mechanism in this class of steels, but certain alloy elements, notably nickel, can be used to advantage to promote a homogeneous slip character.

The predominant failure mode in pipelines is rapid, unstable shear-crack propagation. The crack extension mechanism is one of repeated nucleation of internal voids (usually at second-phase particles) and coalescence of the voids by plastic strain. In line pipe steel the most important void-nucleation sites are the non-metallic inclusions, but with increasing

strength level the second-phase transformation products (carbides, nitrides, etc.) become increasingly important. The volume fraction of internal voids, for a given strain, can be reduced by:

1. reducing the inclusion content,
2. making the inclusions more equiaxed,
3. reducing the carbon content,
4. ensuring that the second-phase transformation products are homogeneously distributed and equiaxed,
5. refining the ferrite grain size.

Given the best relation between strain and the volume fraction of internal voids that can be obtained, the strain at which the voids link up and, hence, the fracture toughness, is determined by the plastic deformation behaviour of the ferrite matrix. The highest toughnesses should be associated with a homogeneous slip character and a high rate of work hardening.

REFERENCES

1. "Metallurgy of High-Strength Low-Alloy Pipeline Steels: Present and Future Possibilities", J. M. Gray, Molybdenum Corporation of America Report No. 7201 (1972).

2. "Steel Developed for Arctic Gas Lines", J. L. Mihelich and J. H. Smith, Oil and Gas Journal 70, 49 (June 19, 1972).

3. "Manganese-Molybdenum-Niobium Acicular Ferrite Steels with High Strength and Toughness", Y. E. Smith, A. P. Coldren, and R. L. Cryderman, in Toward Improved Ductility and Toughness, Climax Molybdenum Development Co. (Japan) p 119 (1971).

4. "Controlled Rolling of Structural Steels", J. Irvine, T. Gladman, J. Orr, and F. B. Pickering, J. Iron and Steel Inst. 208, 717 (1970).

5. "Mild Steels", W. E. Duckworth and J. D. Baird, J. Iron and Steel Inst. 207, 854 (1969).

6. "The Development of High-Strength Structural Steels", K. J. Irvine, in Strong, Tough Structural Steels, ISI Spec. Report No. 104, p 1 (1967).

7. "Advantages and Economics of Quenched and Tempered Weldable High-Strength Steel", J. Lessells and J. Sinclair, J. Iron and Steel Inst. 205, 249 (1967).

8. "Quenched and Tempered Plate Steels", T. F. Pearson and M. de Lippa, J. Iron and Steel Inst. 205, 257 (1967).

9. "A New Heat Treated Constructional Steel", J. C. Bomberger, D. L. Freyberger, and E. L. Fogleman, Met. Prog. 86, 82 (Dec. 1964).

10. "The Heat Treatment of Steel Plates", J. Lessells, J. West Scotland Iron and Steel Inst. 74, 49 (1966)

11. "Development in Equipment and Practices for Quenching Steel Plates", G. F. Melloy, C. W. Roe, and R. D. Romeril, Iron and Steel Engineer 43, 128 (Dec. 1966).

12. "Quenched and Tempered Low-Carbon Steels", J. J. Irani and G. Tither, in Strong, Tough Structural Steels, ISI Spec. Report No. 104, p 135 (1967).

13. "Structure of Metals", C. S. Barnett and T. B. Massalski, McGraw-Hill, p 486 (1966).

14. "Physical Properties of Martensite and Bainite", ISI Spec. Report No. 93 (1965).

15. "Observations on Surface Relief Effects Associated with the Formation of $\theta(CuAl_2)$ Rods in Al-4.5 Wt Pct Cu", H. McI. Clark and C. M. Wayman, Met. Trans. 3, 1979 (1972).

16. "An Edge-Quenching Apparatus for Determining the Effect of Cooling Rate on the Mechanical Properties and Microstructures of Steels", W. B. Davis, C. C. Earley, and E. A. Almond, J. Iron and Steel Inst. 210, 501 (1972).

17. "Yield Strength and Transformation Substructure of Low-Carbon Martensite", G. R. Speich and H. Warlimont, J. Iron and Steel Inst. 206, 385 (1968).

18. "Quenched and Tempered Low-Carbon Steels Containing Niobium or Vanadium", J. J. Irani, D. Burton, and F. Keyworth, J. Iron and Steel Inst. 204, 702 (1966).

19. "The Tempering of a Low-Carbon Internally Twinned Martensite", C. J. Barton, Acta Met. 17, 1085 (1969).

20. "The Morphology of Iron-Nickel Massive Martensite", J. M. Marder and A. R. Marder, ASM Trans. Quart. 62, 1 (1969).

21. "Martensite Transformation in Low-Carbon Steels", J. M. Chilton, C. J. Barton, and G. P. Speich, J. Iron and Steel Inst. 208, 184 (1970).

22. "Transformation Characteristics of Low-Carbon Steels Containing 5 Pct Ni", J. M. Chilton and G. R. Speich, Met. Trans. 1, 1019 (1970).

23. "High-Carbon Bainitic Steels", K. J. Irvine and F. B. Pickering, in Physical Properties of Martensite and Bainite, ISI Spec. Report No. 93, p 110 (1965).

24. "The Formation of Low-Carbon Martensite in Fe-C Alloys", A. R. Marder and G. Krauss, ASM Trans. Quart. 62, 957 (1969).

25. "The Morphology of Martensite in Iron Alloys", G. Krauss and A. R. Marder, Met. Trans., 2, 2343 (1971).

26. "Heat Treatment of Low-Carbon Steels", N. P. Allen and R. Priestner, in Heat Treatment of Metals, ISI Spec Report No. 95 (1966), P.1.

27. "An Apparatus for the Direct Quenching of Steel Plate", M. J. Stewart and J. A. Perry, Mines Branch Internal Report PM-M-72-7 (July 1972).

28. "Properties of Directly Quenched and Tempered Structural Steel Plate", G. Tither and J. Kewell, J. Iron and Steel Inst. 208, 686. (1970).

29. "The Benefits of Direct Quenching After Hot Deformation", G. Tither and J. Kewell, in Proc. of the 2nd International Conference on Strength of Materials, ASM, p 910 (1971).

30. "Microstructure and Mechanical Properties of Some Direct-Quenched and Tempered Low-Carbon Steel", G. Tither and J. Kewell, J. Iron and Steel Inst. 209, 482 (1971).

31. "Recrystallization Kinetics of Martensitic Extra-Low Carbon Steels", A. Galibois and A. Dubé, Can. Met. Quart. 3, 321 (1964).

32. "Tempering of Low-Carbon Martensite", G. R. Speich, Trans. AIME 245, 2553 (1969).

33. "Tempered Martensite Brittleness in Extra-Low-Carbon Steels", G. Delisle and A. Galibois, J. Iron and Steel Inst. 207, 1628 (1969).

34. "Carbide Precipitation in Tempered Extra-Low-Carbon Steels", G. Delisle and A. Galibois, Scripta Met. 5, 309 (1971).

35. "A Study of the Tempering of Steel Using Transmission Electron Microscopy", E. Tekin and P. M. Kelly, in Precipitation from Iron-Base Alloys, AIME, p 173 (1965).

36. "Nature of χ Carbide and Its Possible Occurrence in Steels", K. H. Jack and S. Wild, Nature 212, 245 (1966).

37. "The Mechanical Properties of Matter", A. H. Cottrell, Wiley (New York), p 282 (1964).

38. "Precipitation Hardening by Coherent Particles", H. Gleiter and E. Hornbogen, Mat. Sci. and Eng. 2, 285 (1967).

39. "Strengthening of Steel by Second-Phase Particles", R. B. Nicholson, in Effect of Second-Phase Particles on the Mechanical Properties of Steels, Iron and Steel Inst. Spec. Report No. 145, p 1 (1971).

40. "Effect of Mn and Ni on Impact Properties of Fe and Fe-C Alloys", W. Jolley, J. Iron and Steel Inst. 206, 170 (1968).

41. "Influence of a 3.28 Pct. Ni Addition on the Yield and Fracture Behavior of Alpha Iron", W. Jolley, Trans. AIME 242, 306 (1968).

42. "Fracture Toughness of Materials", G. T. Hahn, M. F. Kanninen, and A. R. Rosenfield, to be published in Annual Review of Materials Science 2, (1972).

43. "Full-Scale Studies", A. R. Duffy, in Symposium on Line Pipe Research, American Gas Assoc. (New York), p 43 (1965).

44. "Recent Work on Flaw Behavior in Pressure Vessels", A. R. Duffy, R. J. Eiber and W. A. Maxey, in Practical Fracture Mechanics for Structural Steel, M. Dobson ed. U.K.A.E.A., p M1 (1969).

45. "Applications of the Instrumented Charpy Impact Test", R. A. Wullaert, in Impact Testing of Metals, ASTM STP 466 p 148 (1970).

46. "Some Effects of Microstructure on the Fracture of Steel", D. E. Osborne, M. Eng. Thesis, McMaster University (1972).

47. "Fracture of Steels Containing Pearlite", A. R. Rosenfield, G. T. Hahn, and J. D. Embury, presented at the AIME-IMD Symposium on The Cellular and the Pearlite Reactions, Detroit, (1971) to be published in Met. Trans.

48. "Deformation of Plastically Non-Homogeneous Materials", M. F. Ashby, Phil. Mag. 21, 399 (1970).

49. "The Effect of Nonmetallic Inclusions on Impact Properties of Steels", T. Saito and I. Uchiyama, Trans. Nat. Res. Inst. for Metals 14, 1 (1972).

50. "Effects of Second-Phase Particles on Strength, Toughness and Ductility", T. Gladman, B. Holmes, and I. D. McIvor in Effect of Second-Phase Particles on the Mechanical Properties of Steel. ISI Spec. Report No. 145, p 68 (1971).

51. G. T. Hahn, unpublished research, Battelle Columbus Laboratories, (1972).

52. "Character of Slip Bands in Iron and a Mild Steel With Manganese", J. D. Boyd, G. T. Hahn, A. R. Rosenfield, and E. Votava, ASM Trans. Quart. 62, 207 (1969).

53. "Effect of Strain Rate on the Dislocation Substructure in Deformed Niobium Single Crystals", J. W. Edington, in Mechanical Behavior of Materials under Dynamic Loads, ed. U.S. Lindholm, Springer-Verlag (New York), p 191 (1968).

54. "Changes in Notch Toughness and Mechanical Properties of Quenched and Tempered Low Carbon Steel Due to Cold Rolling", N. Ujiiye, ISI Japan Trans. 7, 278 (1967).

55. "A. R. Rosenfield, unpublished research, Battelle Columbus Laboratories, (1972).

56. "Effects of Second-Phase Particles on Formability at Room Temperature", D. V. Wilson in The Effect of Second-Phase Particles on the Mechanical Properties of Steel, ISI Spec. Report No. 145, p 28 (1971).

57. "The Environmental Cracking of Line Pipe Steels: A Short Review", G. J. Biefer, Mines Branch Information Circular IC 295, (November 1972).

58. "The Structure and Properties of Bainite in Steels", F. B. Pickering, in Transformation and Hardenability in Steels, Climax Molybdenum Co., (Ann Arbor), p.109 (1967).

JDB/sg